Draft version February 2, 2008
Preprint typeset using LaTeX style emulateapj v. 20/04/00

arXiv:astro-ph/0301162v2 16 Apr 2003

LUMINOUS SUPERSOFT X-RAY SOURCES IN EXTERNAL GALAXIES

R. Di Stefano
Harvard-Smithsonian Center for Astrophysics, 60 Garden Street, Cambridge, MA 02138
Department of Physics and Astronomy, Tufts University, Medford, MA 02155
A. K. H. Kong
Harvard-Smithsonian Center for Astrophysics, 60 Garden Street, Cambridge, MA 02138
Draft version February 2, 2008

ABSTRACT

We use a set of conservative criteria to identify luminous supersoft X-ray sources (SSSs) in external galaxies. We test this approach on blackbody models, and then apply it to *Chandra* data from 4 galaxies: an elliptical (NGC 4967), 2 face-on spirals (M101 and M83), and an interacting galaxy (M51). We find SSSs in every galaxy, and estimate that the total SSS population of sources with $L > 10^{37}$ erg s^{-1} in each galaxy is at least several hundred and could be significantly larger. In addition, we discover two intriguing features of galactic populations of SSSs. First, there are significant subpopulations of high-luminosity sources; the bolometric luminosities can exceed 10^{39} erg s^{-1}. Second, in the spiral galaxies M101, M83 and M51, SSSs appear to be associated with the spiral arms. This may indicate that some SSSs are young systems, possibly younger than 10^8 years.

Subject headings: galaxies: individual (M101,M83,M51,NGC4697) — methods: data analysis — supernova remnants — white dwarfs — X-rays: binaries — X-rays: galaxies

1. INTRODUCTION

Luminous supersoft X-ray sources (SSSs) are characterized by values of kT on the order of tens of eV, and luminosities greater than $\sim 10^{35}$ erg s^{-1}. The corresponding effective radii are comparable to those of white dwarfs (WDs). Indeed, some hot WDs and pre-WDs have been observed as SSSs (see Greiner 2000), including several recent novae, symbiotic systems, and a planetary nebula (PN). More than half of all SSSs with optical IDs, however, do not seem to be examples of systems of known types. It is the mysterious nature of these other systems that has excited much of the interest in SSSs. A promising model is one in which matter from a Roche-lobe-filling companion accretes onto the WD at rates so high ($\sim 10^{-7} M_\odot$ yr^{-1}) that it can undergo quasi-steady nuclear burning (van den Heuvel et al. 1992; Rappaport, Di Stefano & Smith 1992; Hachisu, Kato & Nomoto 1996, Di Stefano & Nelson 1996). Because matter that is burned can be retained by the WD, some SSS binaries may be progenitors of Type Ia supernovae.

There is indirect evidence that nuclear-burning WDs (NBWDs) with a Roche-lobe-filling donor exist in nature. The majority of the SSS binaries whose nature has not yet been determined are considered to be candidates for the "close-binary SSS" (CBSS) model, in which mass transfer is driven on the thermal time scale of a donor whose Roche lobe shrinks as mass transfer proceeds. Nevertheless, studies of the 7 Magellanic Cloud and 2 Milky Way candidates for this or other NBWD models have not yet found direct evidence for the presence of a WD or of a donor. We do know, however, that an X-ray pulsar may present itself an SSS. RX J0059.2-7138 has a non-pulsed luminous ($\sim 6.7 \times 10^{38}$ ergs s^{-1}), soft (~ 30 eV) component (Hughes 1994). Observers outside of the beam of the hard pulsed radiation would classify the source as an SSS. This example serves to illustrate the danger of assuming that all SSSs whose natures we do not yet understand are NBWDs. We also note that the stripped cores of giant stars that have been tidally disrupted by massive black holes are expected to appear as SSSs for times ranging from 10^3 to 10^6 years (Di Stefano et al. 2001). Several such stripped cores could be present within ~ 1 kpc of the nuclei of galaxies harboring high-mass black holes.

Because gas obscures $> 99\%$ of the Milky Way's SSSs, studies of the size and characteristics of galactic populations of SSSs can be carried out only in external galaxies. Here we apply a single set of conservative criteria, applicable to both *Chandra* and XMM data, to identify SSSs in 4 galaxies, allowing direct comparisons of their SSS populations.

1.1. *A Phenomenological Definition of SSSs*

Most SSS spectra are similar to blackbody spectra, although the inclusion of WD atmosphere effects has produced some improved fits. Early definitions of the class assumed $kT < 50$ eV, but this upper limit is unrealistic, since even the flagship SSS CAL 87, has 63 eV $< kT <$ 84 eV (Greiner 2000). In total, 4 of the 9 CBSS candidates have estimated upper limits on kT larger than 50 eV, and 2 also have lower limits above 50 eV, as does the Galactic recurrent nova U Sco, a system which has almost certainly experienced an episode of nuclear burning. There are also theoretical arguments for an upper limit above 50 eV. For example, WDs with masses close to the Chandrasekhar limit are expected to have kT near 100 eV. To derive an extreme upper limit, we note that a $1.4\,M_\odot$ WD with Eddington-luminosity nuclear burning on its surface would have $kT \sim 150$ eV. Because the effective radius is likely to be larger than the radius of the WD, expected temperatures are lower, unless some of these systems can circumvent the Eddington limit.

There is an independent reason to place the division be-

tween SSSs and and other X-ray sources at $kT \sim 175$ eV (Di Stefano & Kong 2003). This is that *Chandra's* detector response (which is similar to that of *XMM* in the soft energy regime), is such that sources below this temperature do not contribute to radiation in the "hard" waveband above 2 keV, while sources with $kT \leq$ 175 eV do exhibit a hard X-ray component (see Di Stefano & Kong 2003).

If there are sources with temperatures greater than $\sim$ 125 eV but less than 175 eV, these are interesting in any case. They could represent (1) an extension of the class of SSSs, (2) low-T supernova remnants (SNRs); these can be distinguished from X-ray binaries through variability studies, or (3) a new class of intermediate temperature X-ray binaries.

The following phenomenological definition selects from the pool of all X-ray sources detected in an external galaxy, the majority of those sources which are SSSs, regardless of their physical nature. An X-ray source is an SSS if either of the following conditions are met. **(1)** The spectrum is well-fit by a blackbody model with $kT < 175$ eV, or **(2)** Whatever the best fit model, fewer than 10% of the energy is carried by photons with energy greater than 1.5 keV. The reason for this condition is that, even if the spectrum starts out as a pure blackbody spectrum, interactions of the radiation with matter near the source, or wind interactions (expected for many SSSs that are quasi-steady NBWDs) can add a small harder component. [1]

Most sources in external galaxies provide too few photons for a meaningful spectral fit. In M101, e.g., 51 of 118 sources provide fewer than 30 photons, 40 sources provide fewer than 25 photons, and 27 provide fewer than 20 photons. It is therefore important to design a uniform procedure to identify those SSSs (the majority) providing fewer than $\sim$ 200 photons. The selection procedure introduced and applied in this paper preferentially selects sources with $kT < 100$ eV.

2. SELECTION CRITERIA

2.1. *The HR Conditions*

In this paper we will employ strict hardness ratio (HR) criteria to identify SSSs. We use 3 energy bins to define hardness ratios: **S:** 0.1-1.1 keV, **M:** 1.1-2 keV, **H:** 2-7 keV. We consider 2 hardness ratios, HR1 and HR2, demanding that

$$HR1 = \frac{M - S}{M + S} < -0.8 \qquad (1)$$

and

$$HR2 = \frac{H - S}{H + S} < -0.8. \qquad (2)$$

These conditions imply that $S > 9\,M$, and $S > 9\,H$.

We also introduce 2 additional hardness ratios that include uncertainties.

$$HR1_{\Delta} = \frac{(M + \Delta M) - (S + \Delta S)}{(M + \Delta M) + (S + \Delta S)} < -0.8, \qquad (3)$$

and

$$HR2_{\Delta} = \frac{(H + \Delta H) - (S + \Delta S)}{(H + \Delta H) + (S + \Delta S)} < -0.8, \qquad (4)$$

where ΔS, ΔM, and ΔH are the one-σ uncertainties in S, M, and H, respectively. Conditions (3) and (4) strengthen the criteria, implying that $(S + \Delta S) > 9\,(M + \Delta M)$, and $(S + \Delta S) > 9\,(H + \Delta H)$. Sources satisfying these 4 conditions are denoted "SSS-HRs".

For sources that do not provide many photons, the precise definitions of $\Delta\,S$, $\Delta\,M$, and $\Delta\,H$ play a crucial role in determining which X-ray sources are tagged as SSS-HRs. There are 2 sources of uncertainty: background, and counting statistics. For each of the 3 bins, we use $\sigma^2 = \sigma'^2(N_S) + N_B$, where N_B is the number of counts extracted from a background region of area equal to that of the source region, N_S is the background-subtracted number of photons extracted from the source region, and $\sigma'(N_S)$ is the one-σ uncertainty in N_S. Since, for *Chandra* observations, the background is generally negligible, the sizes of $\Delta\,S$, $\Delta\,M$, and $\Delta\,H$ can depend primarily on the value of $\sigma'(N_S)$ for each bin. For small values of N_S, $\sigma'(N_S) = 1 + \sqrt{N_S + 0.75}$; for large values of N_S, we have $\sigma'(N_S) = \sqrt{N_S}$. We have chosen to represent $\sigma'(N_S)$ by a function that (1) is exactly equal to the appropriate small-N_S values for $N_S = 0, 1$, (2) approaches $\sqrt{N_S}$, for large N_S, and (3) interpolates between the two at intermediate values. The interpolation formula gives a value of σ near 2 for $N_S < 5$ and closely approximates $\sqrt{N_S}$ for $N_S > 5$

Given these prescriptions, the designation SSS-HR requires that the S band receive more than 13.1 photons if no photons arrive in either the M or H bands, while S must receive more than 24 photons if there is even a single photon in either M or H.

2.2. *Selected Sources*

In cases in which N_H is below $\sim 2 \times 10^{21}$ cm^{-2}, and in which the count rate is high enough that photon statistics do not significantly alter the values of the hardness ratios, the HR conditions will select most SSSs with spectral profiles like those of the nearby SSSs (Greiner 2000). For example, a 100 eV source behind a column of 1.6×10^{20} cm^{-2} will easily satisfy the HR conditions if it provides enough counts. Several circumstances can, however, make this or other true SSSs fail to fulfill the HR criteria. For example, a low count rate, combined with the vagaries of photon statistics will sometimes cause a large enough deficit of photons below 1.1 keV, and a also a large enough excess of photons with energies above 1.1 keV, to cause a true SSS to fail the HR conditions. Thus, as the tests described below illustrate, the HR conditions will select only the strongest candidates SSSs.

2.3. *Tests*

We performed a set of simulations, applying the HR criteria to each of a large number of blackbody sources used to seed galaxies similar to those we will study in §3. Each seeded source was characterized by 3 physical parameters: kT (25 eV $\leq$ $kT \leq$ 2 keV), L ($6.9 \times 10^{35} \leq L_{0.3-7\,keV} \leq 1.4 \times 10^{40}$ erg s^{-1}), and N_H (4×10^{20} erg s$^{-1} \leq N_H < 2.5 \times 10^{22}$ cm^{-2}). We used the PIMMS software (AO3 release) to compute the counts that would be

[1] The choice of 10% is rather arbitrary; future studies of larger numbers of SSSs may suggest that this criterion be altered. For now we allow as much as 10% of the energy to come in at energies above 1.5 keV, because this is roughly consistent with efficient reprocessing or with, e.g., the presence of a companion emitting a strong shocked wind. We do not allow higher values, simply because we want to reserve the SSS classification for sources whose spectrum is clearly dominated by the soft component.

detected in a 50 ksec ACIS-S observation if each physical source were located in a galaxy 5 Mpc, 10 Mpc, and 15 Mpc away. Using PIMMS in ACIS-S mode is equivalent to assuming that each source is located near the center of the backside illuminated S3 chip.

For each physical source and for each energy bin we used 10 values of a random variable r to choose the number of photons detected: $S - 2\,\Delta\,S < S_{detected} < S + 2\,\Delta\,S$, etc. Choosing uniformly over the $\pm 2 - \sigma$ interval slightly overestimates the effects of the uncertainties.

Each galaxy was seeded with 12920 X-ray sources, of which 6080 were SSSs. We applied the HR conditions only to sources that provided more than 14 photons. Figure 1 is a graphical representation of the results for a galaxy located at 10 Mpc, seeded with sources with a maximum luminosity, L_{max}, of 1.4×10^{40} erg s^{-1}. The region for which the selection criteria are most relevant is the one located between the horizontal lines. (The upper horizontal line corresponds to 200 counts. Sources providing more counts can be fit by spectral models, so a selection procedure is less crucial.) Examination of this region reveals that the HR conditions work very well for 55 eV $\leq\ kT \leq$ 100 eV. For low to moderate absorption they select a fair fraction of sources at 25 eV, and 40 eV, and 125 eV, and only a few unabsorbed sources with $kT = 150$ eV.

As Figure 1 indicates, the HR conditions can successfully identify high-count ($>$ 200 count) SSSs with little contamination from non-SSSs. Since, however, the conditions are not strictly needed for these high-count cases, we present in Table 1 test results only for those cases in which the selection procedure can work ($>$ 14 counts) and in which it is needed ($<$ 200 counts). The numbers of SSSs providing between 14 and 200 counts were 1225 for the galaxy at 5 Mpc, 1106 for the galaxy at 10 Mpc, and 1021 for the galaxy at 15 Mpc. In each galaxy, approximately 1/2 of all the seeded SSSs with counts in the range 14−200, were selected as SSSs by the HR conditions. (See Table 1.) Furthermore, among the sources identified as SSS-HRs, the level of contamination was minimal. With more than 500 true SSSs identified as SSS-HRs, there were 4, 7, and 3, outliers mistakenly identified as SSSs in the galaxies at 5, 10, and 15 Mpc, respectively. All of these outliers were located behind small gas columns (4×10^{20} cm^{-2}), had small count rates, and satisfied the HR conditions only because of the effects of limited photon statistics. Most of the outliers had $kT = 175$ eV, while 3 of the 14 had $kT = 200$ eV; thus, even the outliers were remarkably soft X-ray sources.

Examination of both Figure 1 and Table 1 reveal that the HR conditions do have a weakness: they fail to identify a significant fraction of true SSSs. For large values of L_{max} (1.4×10^{40} erg s^{-1}), roughly half of all SSSs sources yielding between 14 and 200 counts were not identified as SSS-HRs. Although the most heavily absorbed sources were most likely to be missed (particularly if kT was near 100 eV), sources with less absorption and low-temperature sources were also missed by the HR criteria. The simulation carried out with a smaller value of L_{max} (1.0×10^{38} erg s^{-1}), demonstrates that the fraction of SSSs not selected is larger for low-luminosity sources, particularly in more distant galaxies, even though only sources providing more than 14 counts were considered.

2.4. *Real Chandra Data*

Chandra's ACIS detectors have suffered degradation at low ($<$ 1 keV) energies. This degradation is time dependent and, as it is presently understood, it was not included in the PIMMS AO3 simulations. In the next section, we apply the selection algorithm to real *Chandra* ACIS-S data taken at different times since 1999. For some of the observations, the AO3 release of PIMMS provides an adequate guide to the flux as a function of temperature and N_H. The progressive low-energy degradation has the effect, however, of making our selection procedures more and more strict when applied to galaxy data taken later and later into *Chandra's* mission. For example, when the effects of the low-energy degradation cause there to be only 2/3 as many counts in the S bin as there would have been in the simulated data, while M and H are relatively unaffected, imposing the requirement that $S > 9\,M$, will be the same as if we had imposed $S > 13.5\,M$ in the simulations. That is, the low-energy degradation makes it more difficult for a true SSS to be identified as such. There is no direct cure for this problem, because we cannot assume that a lack of low-energy photons is due to a lack of sensitivity. Fortunately, even with the degradation, we are able to identify a significant population of SSSs in each galaxy.

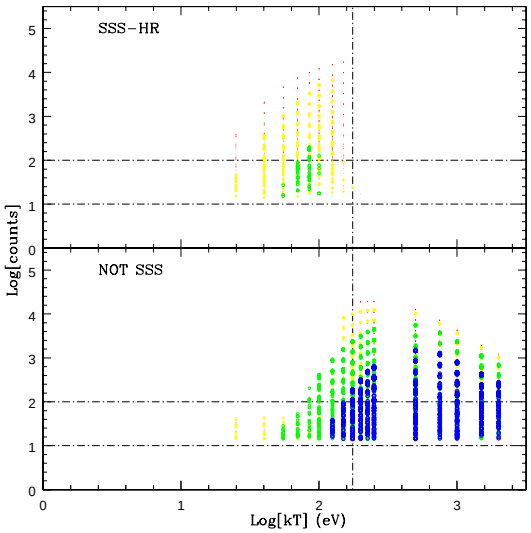

FIG. 1.— Test of the HR criteria as applied to thermal models. Along the vertical axis is the log of the number of counts that PIMMS (AO3 release) predicts would be detected for sources located in a galaxy 10 Mpc away; statistical uncertainties have been included. Source luminosities ranged from 6.9×10^{35} ergs s^{-1} to 1.4×10^{40} erg s^{-1}. Four values of N_H were considered: 4.0×10^{20} cm^{-2} (red points), 1.6×10^{21} (yellow; open circles) cm^{-2}, 6.4×10^{21} cm^{-2} (green; larger open circles), 2.5×10^{22} cm^{-2}(blue; largest open circles). The logarithm of the temperature is plotted along the horizontal axis. Upper panel: points are shown only for those sources that would be identified as SSS-HRs. Lower panel: sources not selected as SSSs by the HR conditions. The first vertical line of sources on the left have $kT = 25$ eV; kT increases by 15 eV through 100 eV, then in 25 eV intervals through to the vertical line at 175 eV, denoting the temperature cut-off for SSSs.

Many distant galaxies are large enough that studies of the X-ray source population must analyze the data taken in all of the chips, not just the backside illuminated chip. For example, a galaxy of diameter 30 kpc, located 10 Mpc away, has dimensions of about 20′, and is therefore spread

TABLE 1
TESTS OF THE HR CONDITIONS

	$L_{max} = 1.4 \times 10^{40}$ erg s^{-1}		$L_{max} = 10^{38}$ erg s^{-1}	
Distance	N_{HR}^{SSS} [a]	$N_{not\ HR}^{SSS}$ [b]	N_{HR}^{SSS} [a]	$N_{not\ HR}^{SSS}$ [b]
D=5 Mpc	598 (4)[c]	627	310 (4)	337
D=10 Mpc	554 (7)	552	147 (3)	212
D=15 Mpc	513 (3)	508	52 (3)	133

For each galaxy distance (rows: 5 Mpc, 10 Mpc, 15 Mpc), two sets of simulations were carried out. In one set of simulations, $L_{max} = 1.4 \times 10^{40}$ erg s^{-1}, where L_{max} is the maximum luminosity of any seeded source. In the second set of simulations, $L_{max} = 10^{38}$ erg s^{-1}.
[a] N_{HR}^{SSS} is the number of SSS-HRs with between 14 and 200 counts.
[b] $N_{not\ HR}^{SSS}$ is the number of SSSs with between 14 and 200 counts *not* identified as SSS-HRs.
[c] The numbers in parentheses are the numbers of sources that are *not* SSSs, but which are identified as SSS-HRs. All such mis-identified sources have $kT \leq$ 200 eV and lie behind small (4×10^{20} cm^{-2}) hydrogen columns.

out over at least 3 chips. Even if the galaxy is smaller or more distant, halo studies would include chips in addition to S3. Unfortunately, however, the soft X-ray sensitivity (which varies somewhat even within S3), is dramatically smaller outside of the backside-illuminated chip. An AO3 ACIS-I observation of a 50 eV (80 eV) source located behind a column of 4×10^{20} cm^{-2}, e.g., will collect only $\sim 14\%$ (20%) as many photons as if the sources were located on-axis in S3. This inevitably implies that some low-flux SSSs will fail to produce a significant detection in the S band. Such sources are lost to any reasonable selection algorithm.

2.5. *XMM Observations*

The HR criteria were designed to optimize the selection of SSSs as simulated by PIMMS for *Chandra* ACIS-S observations. As presently formulated, they will have almost the same effect on data from *XMM*, which offers similar energy coverage but with larger effective area. We compared the sensitivity of *XMM*/PN (with a thin filter) and *Chandra* ACIS-S. For SSSs we found that, in the S, M, and H bands, *XMM* collects ~ 3, ~ 2, and ~ 3 times as many photons as *Chandra*, respectively. This suggests that the primary difference between *XMM*/PN and *Chandra* ACIS-S is that the former has somewhat smaller relative sensitivity to photons in the M band. *XMM* observations of distant galaxies do suffer from significantly more background than *Chandra* observations of the same galaxies. Nevertheless, because of its larger effective area, and also because of the degradation in *Chandra's* low-energy sensitivity, *XMM* may do better in searching for SSSs in regions where source confusion and diffuse gas emission are not problems.

2.6. *Foreground and background objects*

The field of each galaxy contains X-ray sources unrelated to the galaxy, such as background AGN, and X-ray active foreground stars. Given the exposure times of the galaxies we study in §3, we may expect $10 - 15$ foreground/background objects in M51, M83, and NGC 4697 (see, e.g., Soria & Wu 2002; Sarazin, Irwin, & Bregman 2001), and close to 30 in the field of M101 (Pence et al. 2001). For the purposes of this paper, we must estimate the fraction of the foreground and background objects likely to be identified by the HR conditions as SSSs. To make this estimate, we have investigated data from the ChaMP (*Chandra* Multiwavelength Project [2]) archives (P. Green, private communication). In 5 ACIS-S observations with durations $\sim 10 - 20$ ks, no sources satisfied the HR conditions. Therefore, even though there are soft AGN, and even though many X-ray active stars emit soft X-rays, such sources appear unlikely to significantly contaminate the pool of SSS-HR sources.

[2] http://hea-www.harvard.edu/CHAMP

3. APPLICATION TO 4 GALAXIES

We applied the HR conditions to the X-ray sources in 4 galaxies: 3 spirals and an elliptical. Table 2 summarizes key properties of the galaxies, and of the *Chandra* observations. M101 lies along a direction with little Galactic absorption and our view of the galaxy is almost face on; it is therefore an ideal place to search for SSSs. M83 is almost face-on and has experienced recent star bursts. M51 is more inclined, and is interacting with another galaxy. For M101 and M51 we generated our own source lists with the CIAO tool WAVDETECT. For M83 we used a source list provided by R. Soria, and for NGC 4697 we used the source list of Sarazin, Irwin, & Bregman (2001). If the lower limit of the energy range that had originally been used by WAVDETECT was higher than 0.1 keV, we carried out a visual inspection to search for any sources with reliable detections but with few photons detected above 0.3 keV. Details, and complete source lists can be found in Di Stefano & Kong (2003b). We found 33 SSS-HR sources in the 4 galaxies: 3% of the sources detected in NGC 4697 are SSS-HRs, while the comparable fraction for M101 is 15% (see Table 3).

3.1. *Spectra*

Eight sources provided enough photons to allow spectral fits. (Two of these sources permitted spectral fits in each of 2 separate observations.) In NGC 4697, the most distant galaxy, we considered a composite of all 3 SSS-HRs, which happened to have similar spectral profiles in bins of 0.2 keV from 0.1 to 0.7 keV.

Before presenting the results, we note that there is likely to be more systematic uncertainty in fits of SSS spectra

TABLE 2
SUMMARY OF SAMPLE GALAXIES

Name	Type	Distance (Mpc)	D_{25} (arcmin)	Inclination	N_H (10^{20}cm^{-2})	*Chandra* exposure (ks)	M_{BH} ($\times 10^8 M_\odot$)	N_{SSS}/N_{total} [a]
M101	Sc	5.4, 6.7[1]	23.8	0°	1.2	94.4, 9.6[b]	< 0.01 [2]	16/118
M51	Sc[c]	7.7, 8.4[3]	13.6	64°	1.6	14.9, 26.8[b]	0.1 [4]	3/71; 2/92
M83	Sc	4.57[5], 4.7	11.5	24°	3.8	49.5	0.1 [6]	10/128
NGC 4697	E	11.7[7], 15.9[8], 23.3	7.1	44°[d]	2.1	39.3	1.2[9]	3/91

NOTE. — All data are from Nearby Galaxies Catalogue (Tully 1988) unless specified. M101 was observed on 2000 March 26 and 2000 October 29[b]; M51 was observed on 2000 June 20 and 2001 June 23[b]; M83 was observed on 2000 April 29; NGC 4697 was observed on 2000 January 15.

[a] Ratio of number of SSSs to total number of X-ray sources.
[b] The second observation.
[c] Seyfert 2 galaxy.
[d] For elliptical galaxies the inclination is given by $3° + \mathrm{acos}\left(\sqrt{((d/D)^2 - 0.2^2)/(1 - 0.2^2)}\right)$, where d/D is the axial ratio of minor to major diameter (Tully 1988). This inclination angle is generally unrelated to the value of N_H.

REFERENCES. — 1: Freedman et al. 2001; 2: Moody et al. 1995; 3: Feldmeier et al. 1997; 4: Hagiwara et al. 2001; 5: Karachentsev et al. 2002; 6: Thatte et al. 2000; 7: Tonry et al. 2001; 8: Faber et al. 1989; 9: Ho 2002

TABLE 3
SSS-HR SOURCE LIST

Object	R.A.	Dec.	Soft		Medium		Hard		HR1[a]	HR2[b]
	(h:m:s)	(°:′:″)	Counts	S/N	Counts	S/N	Counts	S/N		
M101-15(10)	14:02:59.4	+54:20:42	31.3	5.3	1.3	0.9	0.0	0.0	-0.9(-0.9)	-1.0(-0.9)
M101-18(13*)	14:03:01.1	+54:23:41	169.6	12.9	0.0	0.0	0.1	0.1	-1.0(-1.0)	-1.0(-1.0)
M101-21(16*)	14:03:02.5	+54:24:16	74.2	8.4	0.0	0.0	0.0	0.0	-1.0(-1.0)	-1.0(-1.0)
M101-34(27)	14:03:07.9	+54:21:23	35.7	5.8	1.8	1.2	0.0	0.0	-0.9(-0.9)	-1.0(-1.0)
M101-37(30*)	14:03:08.5	+54:20:57	29.3	5.1	1.0	1.0	0.0	0.0	-0.9(-0.9)	-1.0(-0.9)
M101-38(31)	14:03:08.6	+54:23:36	20.7	4.1	0.0	0.0	0.0	0.0	-1.0(-1.0)	-1.0(-1.0)
M101-43(36)	14:03:10.6	+54:21:26	18.2	3.8	0.0	0.0	0.0	0.0	-1.0(-1.0)	-1.0(-0.9)
M101-50(43)	14:03:13.2	+54:21:57	31.3	5.3	0.0	0.0	0.4	0.3	-1.0(-1.0)	-1.0(-0.9)
M101-51(45*)	14:03:13.6	+54:20:09	219.1	14.6	0.3	0.2	0.0	0.0	-1.0(-1.0)	-1.0(-1.0)
M101-55(48)	14:03:13.9	+54:18:11	34.3	5.6	1.4	1.0	0.0	0.0	-0.9(-0.9)	-1.0(-0.9)
M101-78(73)	14:03:22.6	+54:20:38	34.3	5.3	1.5	1.0	1.0	0.5	-0.9(-0.9)	-0.9(-0.9)
M101-80(75)	14:03:24.0	+54:23:37	68.7	8.0	0.8	0.5	0.0	0.0	-1.0(-0.9)	-1.0(-1.0)
M101-97(92)	14:03:29.8	+54:20:58	71.9	7.7	0.0	0.0	0.0	0.0	-1.0(-1.0)	-1.0(-0.9)
M101-101(96*)	14:03:31.9	+54:23:23	30.9	5.0	0.0	0.0	0.0	0.0	-1.0(-1.0)	-1.0(-1.0)
M101-102(98)	14:03:32.3	+54:21:03	8512.0	92.2	658.4	25.6	68.0	8.0	-0.9(-0.9)	-1.0(-1.0)
M101-102 (2nd obs)			290.2	17	4.7	2.1	0.5	0.5	-1.0 (-1.0)	-1.0 (-1.0)
M101-104(99*)	14:03:33.3	+54:18:00	227.8	14.5	0.3	0.1	1.1	0.3	-1.0(-1.0)	-1.0(-1.0)
M83-20	13:36:53.9	-29:48:48	43.0	5.6	2.6	1.2	2.6	1.0	-0.9(-0.8)	-0.9(-0.8)
M83-42	13:36:59.1	-29:53:36	30.5	5.3	0.0	0.0	0.0	0.0	-1.0(-1.0)	-1.0(-1.0)
M83-50	13:37:00.4	-29:50:54	105.1	10.0	0.8	0.7	0.0	0.0	-1.0(-1.0)	-1.0(-1.0)
M83-54	13:37:01.1	-29:54:49	132.6	11.4	1.8	1.3	0.7	0.7	-1.0(-1.0)	-1.0(-1.0)
M83-79	13:37:06.1	-29:52:32	108.6	10.3	1.9	1.3	0.0	0.0	-1.0(-0.9)	-1.0(-1.0)
M83-81	13:37:06.5	-29:54:16	15.7	3.7	0.0	0.0	0.0	0.0	-1.0(-1.0)	-1.0(-1.0)
M83-88	13:37:07.4	-29:51:33	17.5	3.9	0.0	0.0	0.0	0.0	-1.0(-1.0)	-1.0(-0.9)
M83-98	13:37:12.8	-29:50:12	35.9	5.8	2.1	1.4	1.6	1.1	-0.9(-0.8)	-0.9(-0.9)
M83-111	13:36:59.5	-29:52:03	78.2	8.4	5.9	2.2	2.0	1.3	-0.9(-0.8)	-0.9(-0.9)
M83-128	13:36:57.7	-29:53:53	29.6	5.3	1.6	1.1	0.0	0.0	-1.0(-1.0)	-0.9(-0.8)
M51-12	13:29:43.3	+47:11:34	272.7	16.5	5.2	2.1	1.0	1.0	-1.0(-0.9)	-1.0(-1.0)
M51-12 (2nd obs)			366.0	19.1	11.4	3.4	0.0	0.0	-0.9(-0.9)	-1.0(-1.0)
M51-42	13:29:55.4	+47:11:43	14.7	3.6	0.0	0.0	0.0	0.0	-1.0(-0.9)	-1.0(-1.0)
M51-58	13:30:02.3	+47:12:38	20.4	4.4	0.0	0.0	0.0	0.0	-1.0(-1.0)	-1.0(-1.0)
M51-51 (2nd obs)	13:29:55.3	+47:11:26	14.6	3.4	0.0	0.0	0.0	0.0	-1.0(-1.0)	-1.0(-1.0)
NGC4697-16	12:48:37.1	-05:47:58	63.0	7.9	0.0	0.0	0.0	0.0	-1.0(-1.0)	-1.0(-1.0)
NGC4697-19	12:48:34.5	-05:47:49	73.7	8.5	0.9	0.9	0.0	0.0	-1.0(-1.0)	-1.0(-1.0)
NGC4697-52	12:48:41.2	-05:48:19	58.6	7.5	0.0	0.0	0.7	0.7	-1.0(-1.0)	-1.0(-0.9)

NOTE.— The object ID in parentheses is from Pence et al. (2001); SSSs selected by Pence et al. (2001) are noted by "*".
[a] $HR1 = (M - S)/(M + S)$; value in parentheses is $\mathrm{HR1}_\Delta$. [b] $HR2 = (H - S)/(H + S)$; value in parentheses is $\mathrm{HR2}_\Delta$.

than in the fits of spectra associated with any other class of sources. Calibration issues have not been resolved at the softest energies, introducing obvious anomalies into the spectra of bright nearby SSSs. Most SSSs in distant galaxies provide too few photons for these anomalies to be obvious, yet the calibration problems may influence the derived values of T and L in ways yet to be understood. We proceed anyway, with the caveat that all SSS spectra will need to be revisited once the calibration is complete.

With one exception, blackbody models provided acceptable fits; all values of kT lie between 50 eV and 117 eV, with 2.4×10^{20} cm^{-2} $< N_H <$ 2.14×10^{21} cm^{-2}. (See Table 4.) Thus, applied to real data, the conditions acted as the simulations predict. The single source that required a 2-component fit was M101-102, as observed in its high state during the long observation, yielding $>$ 8000 photons. Even in this state, only $\sim$ 2% of the energy was received in photons with energy $>$ 1.1 keV, validating the selection procedure. Three SSS-HR spectra are shown in Figure 2.

It seems fair to assume that those SSS-HRs which provided fewer counts are good SSS candidates. Indeed, the hardness ratios of all of the SSS-HR sources are well within the limits set by Eqns. 1 through 4; roughly 2/3 of them have HR1=HR2= -1.0.

3.2. *Connections to Previous Work*

SSSs have been selected in 2 of these galaxies by other groups. Sarazin et al. (2001) identified as SSSs all 3 SSS-HRs. Comparison with the work of Pence et al. (2001) on M101 is more difficult. They selected 10 SSSs, but only 7 of them satisfy the HR conditions. While it is not clear why 3 of the SSSs identified by Pence et al. (2001) do not satisfy the HR conditions, it is likely that the 5 SSS-HR sources not selected by Pence et al. (2001) are slightly harder than the sources they targeted. Indeed, the criteria used by Pence et al. (2001) required SSSs to provide 100% of their counts at energies below 0.8 keV, and more than 2/3 of their counts at energies below 0.5 keV (Pence, private communication). The sources in Pence et al. (2001), should therefore preferentially have kT near or below 50 eV. Indeed, the first three sources in Table 2 are M101 sources that were also identified as SSSs by Pence et al. (2001), and all have estimated values of kT below 75 eV. The fourth source in Table 2 is an M101 source that was not identified as supersoft by Pence et al. 2001, presumably because it emits some high-energy photons, in spite of the fact that HR1 and HR2 are -0.9 and -1.0, respectively.

3.3. *Variability*

If the SSSs we discover in other galaxies are X-ray binaries, it is possible for them to exhibit variability on short time scales. Although not every X-ray binary is highly variable, evidence of variability on month-to-year time scales can immediately rule out the hypothesis that the source of the SSS emission is a region as large as $\sim$ 0.1 pc. Note that variability within an observation can be observed for only the brightest SSSs, such as M101-102. In most cases, the detection of variability can best be accomplished by repeated observations of the same galaxy.

Three of the 4 galaxies considered here have been observed twice. M101 (M83) was observed for $\sim$ 100 ksec ($\sim$ 50 ksec) and then again for $\sim$ 10 ksec ($\sim$ 10 ksec). M51 was observed for 15 ksec and 26 ksec. (See Table 2 for the dates of the observations)

3.3.1. *M51*

Because the relative observing times are most similar for the 2 M51 observations, we have created source lists for both observations in order to study the variability of the SSSs. The combination of the 2 observations identified 4 SSS-HR sources, each of which was variable at some level.

One SSS-HR from the 15 ksec observation (M51-58-1) was not detected in the 26 ksec observation; based on the detection of 21 photons in the short observation, we would predict 31 photons in the second observation; none were detected. One SSSs from the longer observation (M51-51-2) was not detected in the shorter observation; 10 counts were predicted in the short observation. M51-42-1 (14.7 counts; all in S) exhibits a clear change; it is detected (49.5 counts; M51-52-2) and is soft in the second observation, but is not an SSS-HR. The brightest SSS in M51, M51-12-1/M51-13-2, decreased in flux by 50% between the observations, and became slightly harder (see Figure 3 and Table 2).

The fact that some level of variability is exhibited by all of M51's SSS-HRs suggests that the majority of SSSs in M51 are not SNRs or other extended emitters.

3.3.2. *M101*

In both M83 and M101, the shorter observation had a duration only 0.1 that of the longer observation; we can therefore check for the variability of only the brightest sources. For the purposes of this paper we have checked the position of each SSS-HR identified in the long observation of M101 to determine if a soft source was detected during the 10 ksec observation. Seven of the 20 SSS-HR sources were detected and were soft during the 10 ksec observation (M101-18, 34, 51, 97, 101, 102, 104). We have not determined whether these 7 sources satisfied the HR condition during the short observation, but we do find that the observed count rates during the short observation were consistent with those taken during the long observation in all but one case. Among the 13 long-observation sources that were not detected in the short observation, the predicted numbers of counts range from 3 to 8. In most cases there were no photons within the PSF. It is very likely that some or even most of the non-detection indicate genuine variability. We can write the probability of the source having the same luminosity as in the long observation but not being detected in the short observation as $0.1\,p_i$, with $p_i < 10$; in most cases $1 < p_i < 5$. The probability, P, that all of thirteen sources actually had similar fluxes to those observed in the first observation is therefore $10^{-4} < P < 10^{-13}$. Additional observations of long duration are required to quantify the level of variability among M101's SSS-HR sources.

One of the most exceptional examples of SSS variability found to date is provided by M101-102. In the long observation it is clearly ultraluminous (see also Mukai et al. 2002). In the short observation the flux has declined by a

TABLE 4
SPECTRAL FITS TO THE BRIGHTEST SSSS

ID	N_H	kT[a]	kT$_{RS}$[b]	χ^2_ν/dof	Flux[c]	L_X[d]	L_{bol}[e]
	(10^{21}cm^{-2})	(eV)	(keV)				
M101-104	$1.16^{+1.08}_{-0.44}$	67^{+8}_{-14}		1.39/9	2.11	0.74, 1.13	3.62, 5.57
M101-51	$2.14^{+0.83}_{+0.19}$	50^{+3}_{-12}		0.57/7	6.19	2.16, 3.32	33.53, 51.62
M101-18	1 (fixed)	71^{+18}_{-19}		0.96/13	1.02	0.35, 0.55	1.61, 2.47
M101-102 (1st)	$1.54^{+0.19}_{-0.31}$	91^{+7}_{-4}	$0.74^{+0.04}_{-0.05}$	1.18/75	82.67	28.8, 44.4	67.94, 104.59
M101-102 (2nd)	$0.95^{+0.67}_{-0.55}$	76^{+11}_{-10}		0.75/8	20.7	7.22, 11.11	35.0, 53.8
M83-50	$0.24^{+0.74}_{-0.24}$	66^{+13}_{-24}		1.24/5	1.14	0.28, 0.30	0.98, 1.03
M83-54	$0.95^{+1.38}_{-0.69}$	71^{+10}_{-16}		0.66/7	2	0.50, 0.53	2.26, 2.39
M83-79	$2.1^{+3.74}_{-1.53}$	86^{+27}_{-30}		0.33/5	4	1, 1.1	2.69, 2.85
M51-12 (1st)	$0.5^{+0.92}_{-0.46}$	102^{+12}_{-16}		1.12/15	6.17	4.38, 5.20	11.86, 14.11
M51-12 (2nd)	$0.6^{+1.8}_{-0.6}$	117^{+26}_{-29}		0.63/9	4.82	3.42, 4.07	9.13, 10.87
NGC4697 (3 sources)	$0.50^{+0.31}_{-0.37}$	81^{+11}_{-7}		0.66/6	1.89	3.10, 12.28	10.72, 42.51

NOTE.— All quoted uncertainties are at the 90% confidence level. The ACISABS model was applied to correct for the low-energy degradation of ACIS (see Kong et al. 2002).
[a] Blackbody temperature.
[b] Raymond-Smith temperature.
[c] Unabsorbed flux ($\times 10^{-14}$ erg cm^{-2} s^{-1}) in 0.3–7 keV.
[d] Luminosity ($\times 10^{38}$ erg s^{-1}) in 0.3–7 keV. The upper and lower limits quoted here are based on the farthest and nearest distances, respectively, shown in Table 2.
[e] Bolometric luminosity ($\times 10^{38}$ erg s^{-1}).

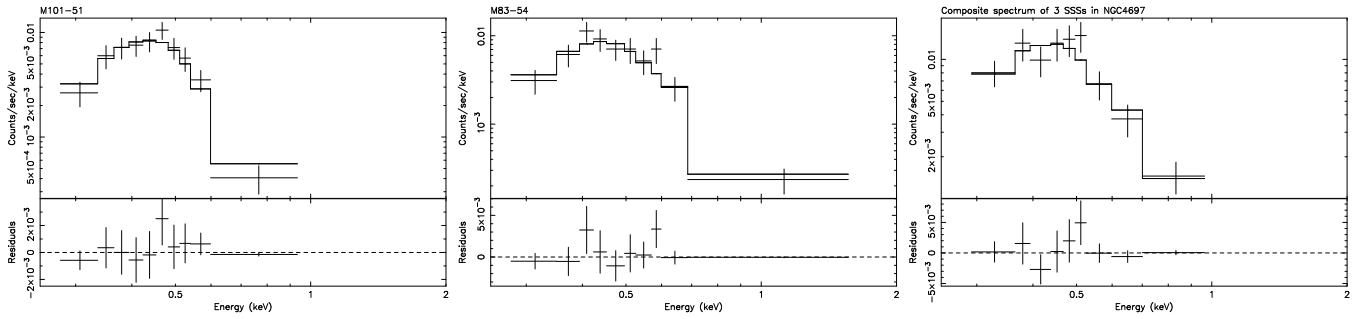

FIG. 2.— Blackbody models for M101-51 ($kT = 50$ eV), M83-54 ($k\ T = 71$ eV) and the composite spectrum of the 3 brightest SSSs in NGC4697 ($k\ T = 81$ eV).

factor of ~ 4, due to a combination of changes in L and T. Furthermore, this source is clearly variable within each observation.

3.3.3. *M83*

The two brightest SSS-HR sources (M83-54 and M83-79) were not detected in the 2001 short observation. Scaling for the exposure time, we would have expected 12-15 counts from each source. The lack of detection does not prove the sources are transient, but does indicate a significant decrease in flux. We note that two non-SSS sources nearby each had a similar number of counts in the long observation, and *are* detected again in the short exposure. See Soria & Wu (2003) for a more detailed discussion of variability in M83.

3.4. *Spatial Distribution*

With our sample of 33 SSSs in external galaxies, it is becoming possible to search for patterns in their spatial distribution within the galaxies; such studies could shed light on the nature and evolution of the sources. Determinations of the relative numbers of SSSs in galactic bulges may allow to us to test the hypothesis that tidal disruption events should produce SSSs that are the hot cores of stripped giants (Di Stefano et al. 2001) There are, however, too few SSS-HRs in the central regions of the 3 spirals studied here to permit meaningful statistical tests at present. Instead we focus on the disk regions, and find an unexpected pattern.

Superposing the positions of the SSSs on optical images of each of the 3 spiral galaxies (Figure 3) produces an impression that a large fraction of the SSSs are in the spiral arms. In most cases, populations found in the spiral arms are young populations, with maximum ages on the order of 10^8 years.

The expected pattern was based on a clear expectation for the nature of the SSSs themselves. Specifically, a large portion of the SSS population was expected to be composed of hot WDs. Since recent novae, hot central stars of PNe and symbiotics have all been observed as SSSs, and in fact comprise nearly half of all SSSs with optical IDs, we expected that at least a fraction of the SSSs in other galaxies should be associated with such systems. In novae and symbiotics, the donor stars are not typically high-mass stars, and they should therefore not presently be associated with young stellar populations. Furthermore, the

most popular model for the remainder of the SSSs also invokes a binary with a slightly evolved donor star with a mass between approximately 1 and 3 $M_\odot$. SSSs described by these models should therefore also be largely associated with populations of old or intermediate-age stars, and should therefore be spread across the face of spiral galaxies, and not found primarily near concentrations of young stars.

In Figure 4 we show the spatial distribution of novae (red circles marked with dates), PNe (yellow crosses) and SSS-HRs (marked red circles) in M101. As expected, the novae and PNe cover the disk of the galaxy. For example, even though there are only 11 novae, several are located away from the arms and also away from regions with bright blue clumps. The same is true of PNe. In contrast, the 16 SSS-HRs are largely absent from these open spaces, and tend to be located within 10″ of bright blue clumps.

At the distance of M101, 10″ corresponds to roughly 200 pc, which is the distance a star traveling at 200 km s^{-1} can cross in 10^6 yrs. If SSS-HRs are young systems, we would therefore expect to find them within $\sim$ 10″ of markers of recent star formation, including bright stars, SNRs, HII regions, and OB associations. Therefore, more convincing than a visual impression of an association between the locations of SSSs and the spiral arms, would be a meaningful statistical correlation between the positions of the SSSs and the positions of markers of young populations. Work is underway to study these correlations in M101 and M83. Below we mention some specific cases in which SSSs are close to optical markers in M101 and M83. The results of a statistical analysis will be reported elsewhere. In M101, one of the SSSs lies within 2″ ($\sim$ 48 pc) of an SNR. Astrometric study is underway to assess the likelihood of a genuine identification. Because the source has a relatively low count rate, we do not have a spectrum.

In addition, 4 distinct SSS-HRs (M101-51,78,80,104), are within 10″ of an HII region. We have spectra for 2 of these sources: M101-104 and M101-51 are among the softest sources in our sample, with kT of 67 eV and 50 eV, respectively.

In M83 one of the SSS-HRs (M83-88) is located within 10″ of an SNR (R. Soria 2002, private communication). The impression that the SSS-HRs are associated with young objects is reinforced by examining their positions relative to clumps in an H_α image of M83 (Figure 4.)

We note that our results are consistent with the only other map of SSSs in a spiral galaxy that we are aware of (Swartz et al. 2002). While we cannot verify that the 9 SSSs on their map satisfy the HR conditions, it is interesting to note that 6 or 7 of these sources appear to be located in the spiral arms.

If indeed we can establish a spatial correlation between SSSs and markers of young stellar populations, and if this correlation is significantly larger than the correlations between PNe (and novae) and markers of young stellar populations, then we will be forced to conclude that a substantial fraction of SSSs are members of relatively young stellar populations. The data so far clearly indicate that the SSSs we are viewing in other galaxies are not primarily members of old or intermediate-age populations.

3.5. *Luminosities*

In most X-ray studies of galaxies, luminosities are estimated for all sources by using a standard spectral model, generally a power law model, to convert the measured count rate to a luminosity. For SSSs, the count rate depends so strongly on the source temperature and on the size of the intervening gas column, that such a simple procedure does not produce meaningful results. We have therefore made luminosity estimates only for the 11 sources for which we have spectral fits (Table 4).

In general, meaningful spectral fits are possible for just a small fraction of all sources in galaxies more distant than 5 Mpc. In NGC 4697, for example, 3% (10%) of all sources provide more than roughly 300 (150) counts; in M101, 14% (24%) of all sources provide more than roughly 300 (150) counts. For SSSs, the effects of absorption can compound those of distance, with low-T sources most affected. A 40 eV, 1×10^{38} erg s^{-1} source, located 8 Mpc away, and observed for 100 ksec by *Chandra's* ACIS-S, will yield approximately 47, 8, and 0.1 photons if N_H is 4×10^{20} cm^{-2}, 1.6×10^{21} cm^{-2}, and 6.4×10^{21} cm^{-2}, respectively. The corresponding numbers of counts for a 55 eV source are 106, 23, and 0.4, respectively. Given these numbers, which were computed with the AO3 release of PIMMS, , it is clear that it will not be possible to obtain spectra for many extragalactic SSSs with $kT < 55eV$. Even higher-temperature SSSs must be very luminous if we are to collect a large number of photons: for an 80 eV 1×10^{38} erg s^{-1} source located 8 Mpc from us, the numbers of counts expected for the 3 values of N_H given above are 227, 75, and 4, respectively.

It is therefore remarkable that we were able to extract spectra for 1/3 of the SSSs found in the 4 galaxies.

3.5.1. *ULSs: Ultraluminous SSSs*

The most luminous SSS in the galaxies we have studied is M101-102. It's luminosity during the long exposure was clearly $> 10^{39}$ erg s^{-1}; thus, by most definitions, it qualified as an ultraluminous X-ray source. M101-102 is an ultraluminous SSS (ULS), and it is the only source in this data set whose X-ray luminosity alone is $> 10^{39}$ erg s^{-1}.

Other sources with bolometric luminosities larger than 10^{39} ergs s^{-1} are M101-51, M51-12 and, the 3 SSS-HRs in NGC 4697 (if the true distance to that galaxy is close to the maximum estimated distance). These sources must, however, be viewed as weaker ULS candidates, since (a) the number of photons received from them was typically more than an order of magnitude smaller than from M101-102, making the spectral fits less certain, and (b) the derived value of the bolometric luminosity is model-dependent.

Even if the estimates of the bolometric luminosities are too high by an order of magnitude (unlikely to be the case for all of the sources), M101-51, M51-12 and the SSS-HRs in NGC 4697 have luminosities near or above the Eddington limit for a 1.4 $M_\odot$ star.

3.5.2. *Sources Near the Eddington Limit*

The estimated bolometric luminosity of 5 additional sources lies near the Eddington limit for a 1.4 $M_\odot$ star. If any of these are NBWDs (whether or not the donor fills its Roche lobe), they are particularly interesting, because

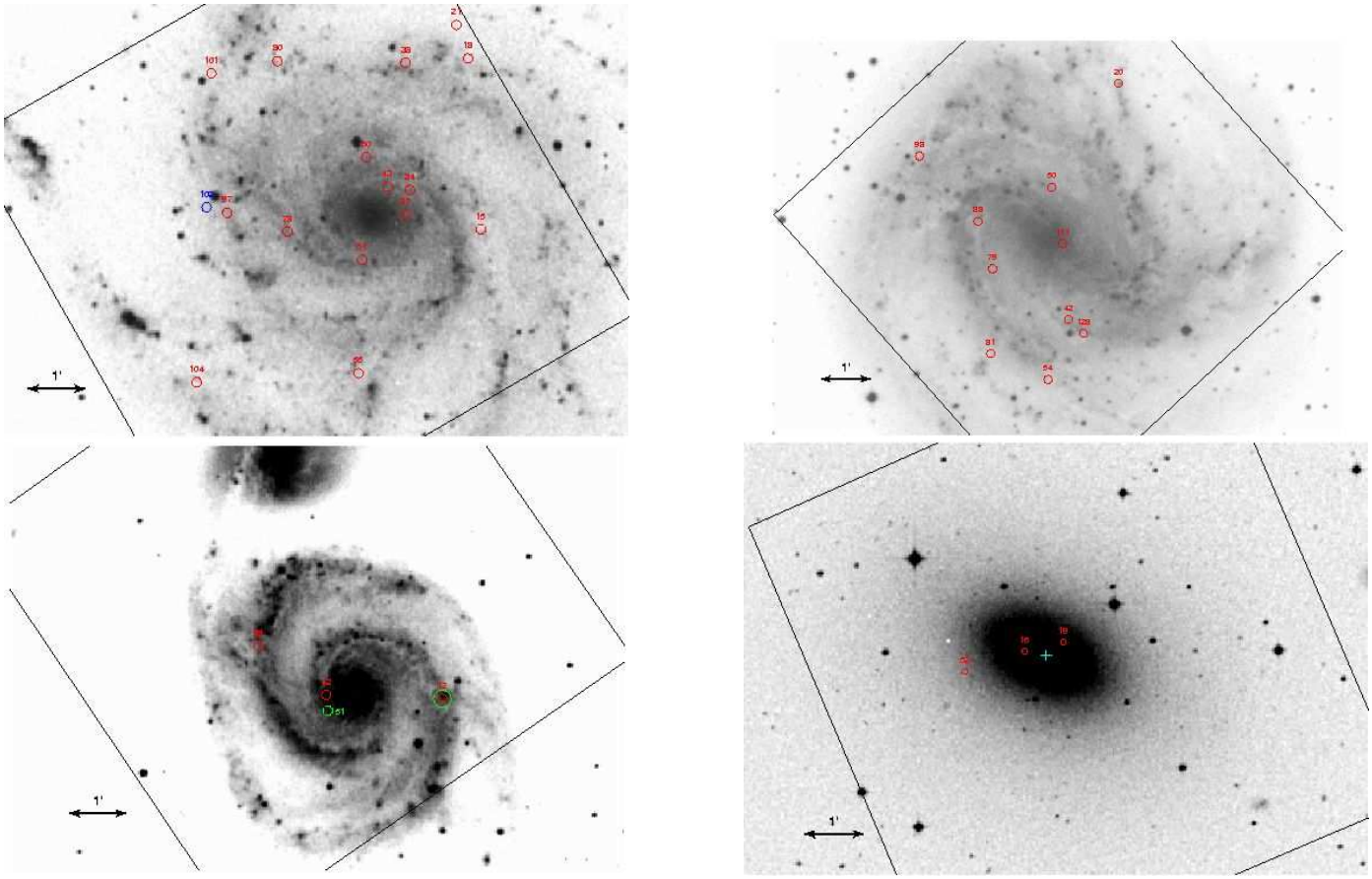

FIG. 3.— *Chandra* field-of-view (ACIS-S3; black line) overlaid on the Digitized Sky Survey images of M101 (upper left), M83 (upper right), M51 (lower left) and NGC4697 (lower right). Also shown in the figures are the positions with source numbers (red circle) of all SSS-HR candidates. The ultraluminous SSS M101-102 is marked by blue circle. In M51, those SSSs found in the second observation are marked by green circle. Note that the central $\sim 10''$ of M51 is excluded. The center of NGC4697 is marked by a blue cross. North is up, and east is to the left.

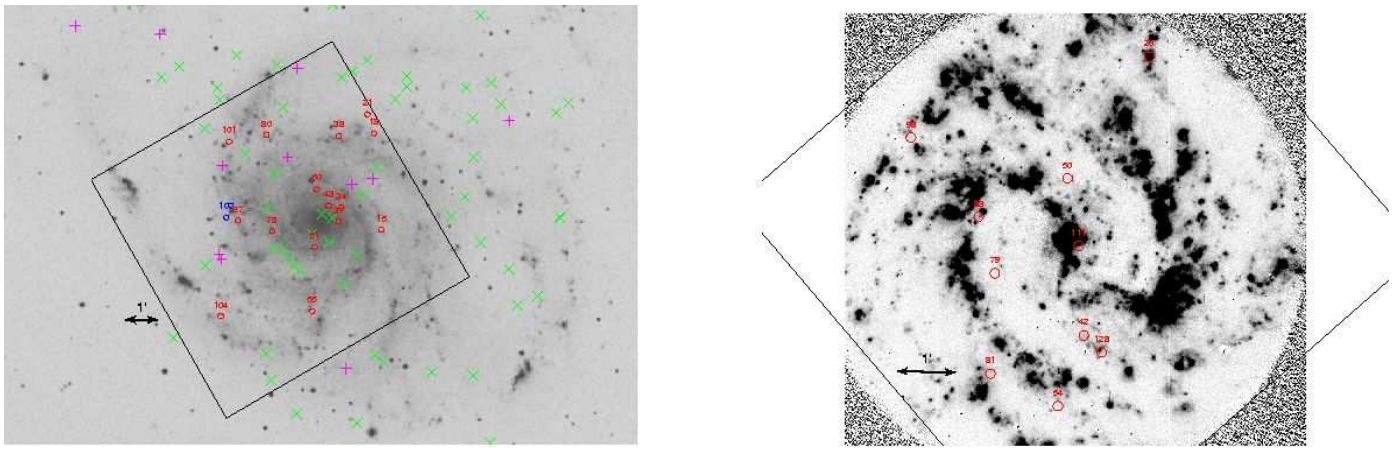

FIG. 4.— Left: The positions of PN (green crosses) and novae (purple crosses) overlaid on the Digitized Sky Survey image of M101. Symbols for SSSs are the sane as Figure 3. Right: Hα image (provided by Stuart Ryder and Roberto Soria) of M83 with positions of SSSs overlaid (symbols same as Figure 3). North is up, and east is to the left.

they could be Type Ia supernova progenitors with masses near the Chandrasekhar limit.

3.5.3. *Sources of Moderate Luminosity*

Two-thirds of the SSS-HRs provided only between 14 and 80 counts, with almost half of them providing fewer than 30 counts. Scaling from the high-L systems, and taking the detection limit for each galaxy into account, it is likely that typical SSS-HRs in our sample have luminosities in the range of a few times 10^{37} to 10^{38} erg s^{-1}. That is, unless their temperatures are considerably lower than 50 eV, or the intervening column is large, their luminosities are similar to the luminosities of the local SSSs discovered

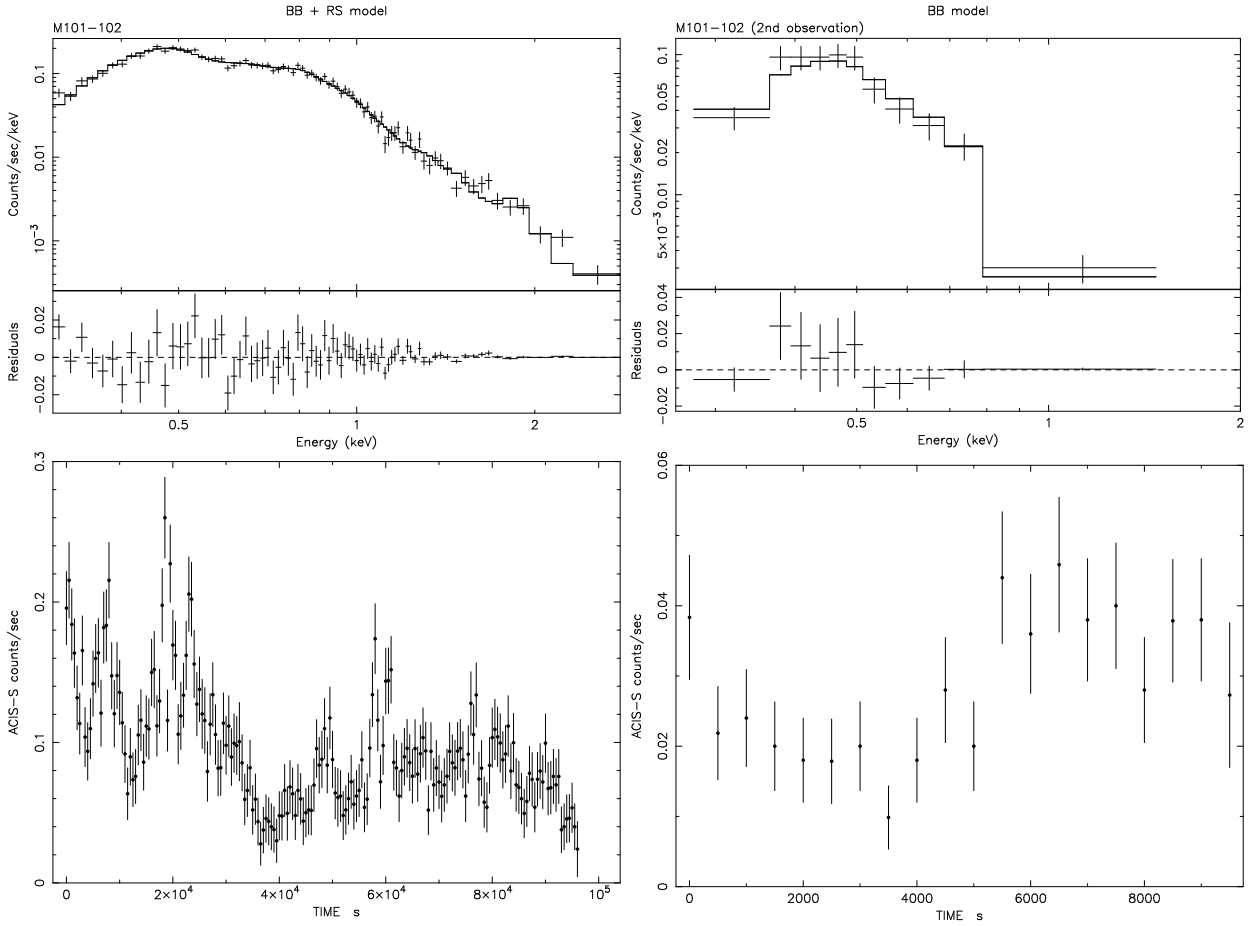

FIG. 5.— X-ray spectra for M101-102 during the first observation (upper left; blackbody plus Raymond-Smith model)) and second observation (upper right; 79 eV blackbody model). Lower panel is the 0.3-7 keV lightcurves (500 s time resolution) of the same sources. Note that the vertical axes have different scales.

during the early years of ROSAT.[3]

3.6. *Total galactic populations*

Based on a small number of ROSAT-identified SSSs, galactic populations of SSSs were estimated to be large, with ~ 1000 $L > 10^{37}$ ergs s^{-1} sources in spiral galaxies such as the Milky Way and M31 (Di Stefano & Rappaport 1994; Motch, Hasinger & Pietsch 1994). In addition, populations numbering in the hundreds had been conjectured to explain the diffuse soft X-ray emission in some elliptical galaxies (Fabbiano, Kim, & Trinchieri 1994).

Because of the effects of absorption, the SSS-HRs we have detected in each galaxy comprise a small fraction of all of the SSSs within the galaxy. We detect primarily the hottest, brightest SSSs. This effect becomes even more pronounced for distant galaxies and/or for (a) galaxies located along lines of sight with large values of N_H, (b) galaxies with large internal gas components, or (c) spiral galaxies with large inclination angles.

To estimate the size of the total population, we must determine what fraction of all the sources we can (1) detect and (2) identify as SSSs. The second requirement is more restrictive, as typically more than 14 photons are needed. Assuming that at least 14 photons are needed we can compute, for each temperature and each value of N_H, the minimum luminosity of a detectable SSS in each galaxy. We have done these computations for each value of T and N_H used in the PIMMS simulations described in §2.

We have then seeded each of the 4 galaxies with the populations of SSSs used by Di Stefano & Rappaport (1994) to estimate the fraction of SSSs that the *ROSAT All-Sky Survey* had discovered in the Galaxy, M31, and the Magellanic Clouds. This tells us the fraction of all "classical" SSSs ($kT < 100$ eV, 10^{37} erg s^{-1} $< L < 2 \times 10^{38}$ erg s^{-1}), that can be detected and identified as SSSs in each galaxy. We have assumed that, if we receive 14 photons from a true SSS, there is a probability of 1/2 that it will identify the source as an SSS-HR, hence as an SSS.

M101 and M83: The fraction of sources we would detect and identify as an SSS ranged from 1% to 2.5%, with a median value of 1.5%. This implies that each "classical" SSS detected represents between 40 and 100 M101 SSSs, with a median expectation value of ~ 66. If we assume that roughly half of the SSS-HR sources in each of these two galaxies represent "classical" SSSs, then the number of "classical" SSSs in each galaxy must lie between 200 and 800.

M51 and NCG 4697: Because of the greater distance to

[3]There are a subset of local SSSs that are associated with CVs; these, like the nova-like variable V751 Cyg (Greiner et al. 1999), are less luminous. Such sources, recognized as SSSs only in recent years, are below our detection threshold.

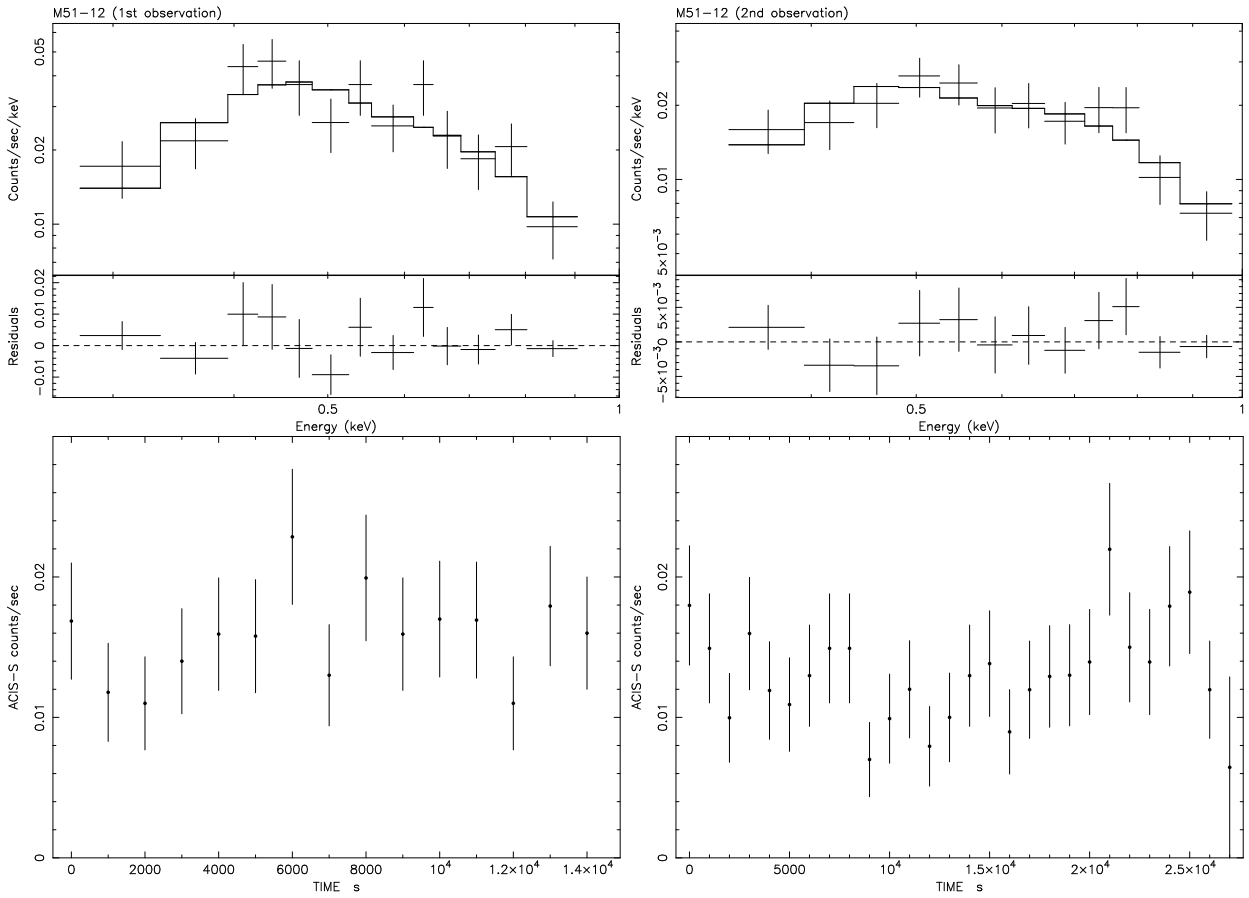

FIG. 6.— X-ray spectra for M51-12 during the first observation (upper left; 102 eV blackbody model) and second observation (upper right; 117 eV blackbody model). Lower panel is the 0.3-7 keV lightcurves (1000 s time resolution) of the same sources.

these two galaxies (particularly for NGC 4697), and because of the relatively high inclination of M51, we can detect a much smaller fraction of all "classical" SSSs in these galaxies. We compute that the fraction of detectable SSSs lies between 0.05% and 0.12% for M51 and between 0.03% and 0.1% for NCG 4697. If, therefore, even one of the SSS-HRs in each galaxy corresponds to a "classical" SSS, the underlying population of SSSs in these galaxies is large, likely to be on the order of 1000. We note that, especially for these galaxies, it is difficult to judge whether the few SSS-HRs we have identified are similar to the classical systems, or if they belong to a hotter and more luminous subclass of SSSs. Even in the latter case, however, it is unlikely that the entire population of SSSs happens to have luminosities and temperatures high enough to bring them over the detection limit. It is therefore all but certain that the SSS population consists of a significantly larger number of sources than we have been able to detect.

In all cases, a large portion of the population of SSSs, the portion corresponding to low luminosities ($<\sim 10^{37}$ erg s^{-1}) and/or low-temperatures ($kT <\sim 30$ eV), is unconstrained. It is therefore worth noting that, in our galaxy, some CV systems have been identified as low-L SSSs; the numbers of such systems in our own Galaxy may be ten times larger than the numbers of "classical" SSSs. In galaxies beyond the Local Group, we can only hope to detect such sources indirectly, e.g., by observations of diffuse soft emission.

In order to improve the estimates for that portion of the SSS population (the hotter and more luminous sources) that *can* be directly detected and/or constrained through *Chandra* and *XMM* observations, several steps, including the following, can be taken: (1) more sensitive sampling of the values of N_H in the simulations, (2) measurements of N_H in the galaxies, tying the location of the detected sources to the local values of N_H.

At present it seems likely that each of the galaxies we have studied houses a population of SSSs that consists of at least a few hundred sources with $L > 10^{38}$ erg s^{-1}. . Additional observations and more sophisticated analyses will improve this estimate.

4. INTERPRETATION

4.1. *The HR Conditions*

Supersoft X-ray sources form a large and intriguing component of galactic X-ray source populations. As *Chandra* and *XMM* discover more SSSs in external galaxies, comparative studies will provide important clues to the natures and physical characteristics of the sources. Such studies require a uniform selection procedure. In this paper we take a first step toward developing a systematic procedure to select SSSs from a galactic population of X-ray sources.

In the absence of a single well-tested physical model, we start with an empirical spectral definition of SSSs. Our definition (§1.1) includes all X-ray sources emitting 90% of their flux in photons with energies < 1.1 keV.

To identify SSSs in external galaxies, selection criteria are needed to assess sources providing too few counts for meaningful spectral fits–i.e., the vast majority of all sources. In this paper we have introduced a strict set of criteria, the "HR conditions", which preferentially select SSSs with $k\ T < 100$ eV. Indeed, SSS-HR's, i.e., sources satisfying the HR conditions, should have spectral characteristics most similar to those of the SSSs discovered locally (in the Magellanic Clouds and Milky Way), with limited contributions from sources with $kT > 100$ eV and virtually no contamination from sources with $kT > 175$ eV.

The clear advantage of the HR conditions is that they are conservative. We therefore expect that applying them will provide insight into the nature of sources with spectra like those of the flagship sources discovered so far in the Magellanic Clouds and Milky Way. In some ways, the study of SSS-HRs in 4 galaxies has verified expectations based on the local sample of SSSs, but this study has also produced some surprises.

4.2. *Results from* 4 *galaxies*

Applying these conservative conditions to *Chandra* data from 4 galaxies allows us to establish that SSSs are an important component of galactic X-ray binary populations. Based on observations of $3-16$ SSS-HRs in each of the 4 galaxies we studied, we estimate that the minimum number of SSSs with $L_x > 10^{37}$ erg s^{-1} in typical galaxies is likely to be in the hundreds. The numbers of lower-L sources remain unconstrained by the observations carried out to date. In addition we appear to have discovered a sub-population of more luminous SSSs that are not present in the Magellanic Clouds and Milky Way.

4.2.1. *The most luminous SSSs*

The spiral galaxies in our sample, and perhaps the elliptical as well, appear to house small populations of SSSs that are ultraluminous. These ULSs could very well be accreting intermediate-mass BHs. Their luminosities and temperatures are consistent with what is predicted for accreting BHs with masses between roughly $100\,M_\odot$ and $1000\,M_\odot$.

Others of the sources appear not to be ultraluminous, but do have luminosities that are near-Eddington or super-Eddington for a $1.4\,M_\odot$ object. Some of these could be accreting WDs with masses approaching the Chandrasekhar mass (Di Stefano 2003, in preparation).

4.2.2. *Young SSSs?*

The spatial distribution of SSS-HRs is not consistent with a population dominated by old stellar systems. At present it seems likely that, at least in spiral galaxies, the population of SSSs includes some systems with ages $< 10^8$ years. While some SNRs may exhibit SSS-like emission, the SSS-HRs which we have been able to test for variability appear not to be SNRs. At least a significant fraction are therefore likely to be X-ray binaries.

The age of a binary when it emits X-rays is generally determined by the age of the donor star when it either fills its Roche lobe or emits a large enough stellar wind that its compact companion can receive mass at rates in the range $10^{-9}-10^{-7} M_\odot$ yr^{-1}. A Roche-lobe filling donor can transfer mass at these rates to a WD in a dynamically stable way only if it is not too much more massive than the WD. Masses of $\sim 1-3 M_\odot$ are allowed. Such systems should not be primarily associated with the spiral arms. In order for such rates to be achieved when the mass transfer occurs through a stellar wind, the donor must be very evolved. Only stars with masses greater than $\sim 5\,M_\odot$ can become so evolved in times shorter than 10^8 years. If the accretor is a WD, the system would be a symbiotic; symbiotics typically have donors of lower mass (see Kenyon 1986). On the other hand, high-mass X-ray binaries (HMXBs) in which the donor is a high-mass star and the accretor is a neutron star or BH are well known. Indeed, the X-ray pulsar with the luminous soft component, RX J0059.2-7138, has been conjectured to be an HMXB (Hughes 1994). It is very likely, therefore, that at least some SSSs found near star-forming regions have BH or neutron star accretors.

4.3. *Status of the WD Models*

Although the spatial distribution of SSSs in the galaxies we have studied so far appears to be indicative of a younger population than we expected to find, it would be premature to conclude that the WD models of SSSs are not correct. It seems more likely that we have discovered new populations that supplement those we had hoped to find.

For example, within our own Galaxy, we would be unable to discover soft sources, even luminous soft sources, located in star forming regions. This study of M101, M83, and M51, which are all located behind relatively small gas columns, and which are less inclined than M31, has provided the first opportunity to systematically search for SSSs among young stellar populations.

Even if our conjecture is correct, i.e., some of the SSSs we have discovered are not hot WDs, some SSSs in these 4 galaxies could be hot WDs. Further observations and even work with existing data may be able to determine the relative contributions of SSSs in young and old stellar systems. (See §5.2.)

5. PROSPECTS

5.1. *Selection Criteria*

If the fact that the HR conditions are conservative selectors of SSSs is their strength, it is also a weakness that prevents them from identifying a significant fraction of all SSSs. In tests based on simulations, the HR conditions fail to select about 1/2 of all SSSs. (See Table 1 and Figure 1.) The fraction of missed SSSs could be larger, and in fact is almost certainly progressively larger in *Chandra* observations taken progressively later than the time of launch. The number of photons in the S band will, by 2004, be a factor of 5 smaller for some sources than predicted in the simulations we have used. (See the recent AO5 PIMMS release: for a hydrogen column of 4×10^{20} cm^{-2}, the S counts predicted for AO5 are 16%, 21%, and 30% of what they were in the AO3 predictions for a 40 eV, 55 eV, and 85 eV source, respectively.) Clearly a more comprehensive set of criteria are needed. We will return to this issue in a separate paper (Di Stefano & Kong 2003).

5.2. *The Physical Nature of SSSs*

This first comparative look at SSSs in external galaxies raises intriguing questions about the nature of the sources. The following observations will help determine the answers.

(1) Repeated X-ray observations. These will allow us to (a) test the hypothesis that some of the SSSs are SNRs, (b) identify SSSs which are recent novae, (c) determine the duty cycles of SSSs which are X-ray binaries, and to (d) discover SSSs of lower luminosity by merging multiple images. We note that *Chandra* observations should be conducted as soon as possible to avoid the worst effects of the degradation in low-energy sensitivity.

(2) Repeated observations at optical and UV wavelengths. These could identify novae and any other events associated with SSS behavior. They also provide the data necessary to study the stellar populations with which SSSs are associated.

(3) Correlation studies. It is difficult to establish optical IDs at distances of several Mpc, since $1''$ corresponds to roughly $4\,D$ pc, where D is the distance to the galaxy, expressed in units of Mpc. Nevertheless, we can hope to establish the types of stellar populations that tend to be associated with SSSs. Preliminary studies of M101 and M83, for example, seem to indicate that the positions of SSSs are more strongly correlated with markers of young stellar populations than are the positions of recent novae, but that they are less correlated with some markers of young stellar populations than the markers among themselves (e.g., the correlation between SNR and HII regions may be stronger than the correlation between SSSs and HII regions). While these effects have yet to be quantified, they might suggest that some SSSs are members of young populations, while others are, as expected, members of older stellar populations. Furthermore, if SSSs tend to be associated with objects that have special optical properties (e.g., if SSSs are bright in UV), then it might be possible to establish some IDs. If, for example, 5 SSSs in one galaxy are associated with UV bright regions, the probability that this is a chance occurrence can be assessed. If it is small, then it is likely that some of the associations are real. We can then compare with IDs that have been established for local SSSs, to determine if the types of objects with which SSSs in distant galaxies are associated are similar to those associated with local and better studied SSSs.

The combination of these steps taken over an interval of years will help us to understand the physical nature of the various sub-populations that comprise the class of luminous supersoft X-ray sources.

We are grateful to Jochen Greiner, Roy Kilgard, Miriam Krauss, Koji Mukai, William Pence, Paul Plucinsky, Andrea Prestwich, Douglas Swartz, Roberto Soria, Harvey Tananbaum, Kinwah Wu, and Andreas Zezas for stimulating discussions and comments. We thank Roberto Soria for providing pre-publication source lists for M83. We are grateful to Paul Green and the ChaMP collaboration for providing blank field source data. This research has made use of the electronic catalog of supersoft X-ray sources available at URL http://www.aip.de/∼jcg/sss/ssscat.html and maintained by J. Greiner. RD would like to thank the Aspen Center for Physics for providing a stimulating environment, and the participants of the workshop on *Compact Object Populations in External Galaxies* for insightful comments. This work was supported by NASA under AR1-2005B, GO1-2022X, and an LTSA grant, NAG5-10705.

REFERENCES

Di Stefano, R., Greiner, J., Murray, S., Garcia, M. 2001, ApJ, 51, L37
Di Stefano, R., Nelson, L.A. 1996, in Supersoft X-Ray Sources, Proceedings of the International Workshop Held in Garching, Germany, 28 February - 1 March 1996. Lecture Notes in Physics, Vol. 472, edited by Jochen Greiner. Springer-Verlag, Berlin Heidelberg New York, 1996., p.3
Di Stefano, R., Rappaport, S. 1994, ApJ, 437, 733
Di Stefano, R. & Kong A.K.H. 2003, ApJ, in preparation
Fabbiano, G., Kim, D.-W., Trinchieri, G 1994, ApJ, 428, 555
Faber, S.M., Wegner, G., Burstein, D., Davies, R.L., Dressler, A., Lynden-Bell, D., Terlevich, R. J. 1989, ApJS, 71, 173
Feldmeier, J.J., Ciardullo, R., Jacoby, G.H. 1997, ApJ, 479, 231
Freedman, W.L., et al. 2001, ApJ, 553, 47
Greiner, J. 2000, New Astronomy, 5, 137.
Greiner, J., Tovmassian, G.H., Di Stefano, R., Prestwich, A., Gonzalez-Riestra, R., Szentasko, L., & Chavarra, C. 1999, A&A, 343, 183
Hachisu, I., Kato, M., & Nomoto, K. 1996, ApJ, 470, L97
Hagiwara, Y, Henkel, C, Menten, K.M., Nakai, N. 2001 ApJ, 560, L37
Ho, L.C. 2002, ApJ, 564, 120
Hughes, J.P. 1994, ApJ, 427
Karachentsev, I.D., et al. 2002, A&A, 385, 21
Kenyon, S.J. 1986, The Symbiotic Stars, Cambridge University Press
Kong, A.K.H., Garcia, M.R., Primini, F.A., & Murray, S.S. 2002, ApJ, 580, L125
Moody, J. W., Roming, P.W.A., Joner, M.D., Hintz, E.G., Geisler, D., Durrell, P.R., Scowen, P.A., Jee, R.O. 1995, AJ, 110, 2088
Mukai, K., Pence, W.D., Snowden S.L., & Kuntz, K.D. 2002, ApJ, in press (astro-ph/0209166).
Motch, C., Hasinger, G., & Pietsch, W. 1994, A&A, 284, 827
Pence, W. D., Snowden, S. L., Mukai, K., & Kuntz, K. D. 2001, ApJ, 561, 189
Rappaport, S., Di Stefano, R., Smith, J.D. 1994, ApJ, 426, 692
Sarazin, C.L., Irwin, J.A., Bregman, J.N, 2001, ApJ, 556, 533
Swartz, D.A., Ghosh, K.K., Suleimanov, V., Tennant, A.F., & Wu, K. 2002, ApJ, 574, 382
Soria, R. & Wu, K. 2002, A&A, 384,99
Soria, R. & Wu, K. 2003, A&A, submitted
Thatte, N., Tecza, M., & Genzel, R. 2000, A&A, 364, L47
Tonry, J.L., Dressler, A., Blakeslee, J.P., Ajhar, E.A., Fletcher, A.B., Luppino, G.A., Metzger, M.R., & Moore, C.B. 2001, ApJ, 546, 681
Tully, R.B. 1988, in Nearby Galaxies Catalog, Cambridge and New York, Cambridge University Press,
van den Heuvel, E.P.J., Bhattacharya, D., Nomoto, K., & Rappaport, S.A. 1992, A&A, 262, 97